Electronic Supplementary Material (ESI) for MedChemComm.

Supporting Information

Effect of Isouronium/Guanidinium Substitution on the Efficacy of a Series of Novel Anti-Cancer Agents

Viola Previtali, Cristina Trujillo, Rebecca Amet, Daniela M. Zisterer, Isabel Rozas*

Table of Contents

1. Computational Studies

We have previously studied the interactions between some arylguanidinium systems and the phosphate groups of ATP to understand their possible mode of action in kinase inhibition. Hence, by characterizing the interactions between the guanidinium cation and the different phosphate groups of the ATP molecule, a theoretical model was proposed.[S1] Now, we present a similar study with 4-phenoxyphenyl-*O*-isouronium (simplified model of the molecules proposed, see Figure 1 in manuscript) interacting with the different ATP phosphates. Due to the size of the ATP molecule we have used DFT level of theory [ωB97XD/6-31+G(d,p)] for a structure optimization and then a single point calculation at MP2/6-311+G(d,p) to obtain accurate binding energies; in both cases the effect of water solvation was accounted for using the SCRF-PCM approach.

In our previous study the most stable interaction between ATP and 4-phenoxyphenyl-*N*-guanidinium[S1] was a simultaneous parallel HB established between two H atoms of the guanidinium moiety and two O atoms of the phosphate. Thus, with the aim of comparing isouronium and guanidinium contacts, only those interactions involving H2 and H3 of the isouronium (see Figure S1) and two O atoms of a phosphate were considered. Given the presence of three phosphate groups in ATP (α, β and γ, Figure S1), the possibility of a 'left' (L), 'right' (R) or 'bottom' (D) interactions from the triphosphate side and 'a' or 'b' orientation of the -O-phenyl moiety with respect to ATP (as represented in Figure S1), a total of 12 possible minima were explored (complexes type **I**, see Table S1).

Hence, different minima were found for interactions by: (i) the right position of the α-phosphate (α-R); (ii) both the right and the left sides of the β-phosphate (β-R and β-L); and (iii) the right, left and bottom position of the γ-phosphate (γ-R, γ-L and γ-D). Moreover, four extra minima were considered, in which an interaction between the 4-phenyloxyphenyl-*O*-isouronium and more than one phosphate is established (complexes type **II**, see Table S1).

Calculated interaction energies (E_i, kJ mol^{-1}) between ATP and 4-phenyloxyphenyl-*O*-isouronium are presented in Table S1; interaction energies with the 4-phenyloxyphenyl-*N*-guanidium cation (in brackets in Table S1) have been included for comparison purposes.

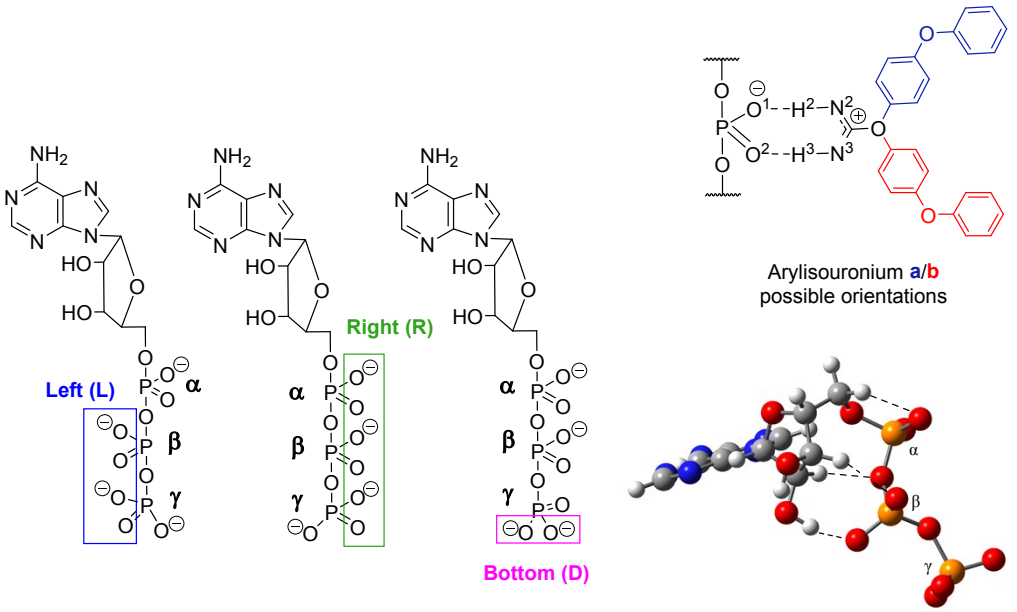

Figure S1. Scheme showing all different positions considered for the interactions between the ATP molecule (left) and the 4-phenyloxyphenyl-*O*-isouronium cation (right up) as well as the isolated ATP molecule optimised at ωB97XD/6-31+G(d,p) and PCM-water computational level showing the intramolecular HBs' net (right bottom).

Table S1. Interaction energies (E_i, kJ mol^{-1}) for the different complexes (type **I** and **II**) formed between arylisouronium or arylguanidinium (values, in brackets, taken from reference S1) with ATP calculated at ωB97XD/6-31+G(d,p)//MP2/6-311+G(d,p) and PCM-water computational level.

		I	**II**
α-R	**[a]**	-117.2 (-105.9)	- -
	[b]	-116.8 (-105.8)	- -
β-R	**[a]**	-141.5 (-129.0)	- -
	[b]	-140.7 (-128.3)	- -
β-L	**[a]**	-101.7 (-95.4)	- -
	[b]	-101.8 (-94.5)	- -
γ-R	**[a]**	-137.6 (-120.6)	-148.6 (-164.4)
	[b]	-135.3 (-119.3)	-153.4 (-160.9)
γ-L	**[a]**	-139.3 (-124.0)	-175.8 (-177.7)
	[b]	-139.5 (-122.5)	-162.3 (-169.3)
γ-D	**[a]**	-181.7 (-163.2)	- -
	[b]	-131.1 (-116.2)	- -

As previously observed for the arylguanidinium complexes, the orientation ([a] or [b]) of the 4-phenyloxyphenyl-*O*-isouronium molecule with respect to the phosphate chain does not seem to be important for the strength of the interaction (ΔE_i around 0.1-2 kJ mol^{-1}) with the exception of the interactions by the bottom side of the γ-phosphate where the di-aromatic system is involved in several interactions with ATP (see Iγ-D[a] in Figure S2). In most cases, the E_i values are larger for the interactions with the γ-phosphate as a result of the more negative character of this group, which in protein kinases is involved in the catalytic mechanism.[S2]

The weak interactions found for the β-L complexes **I** ([a]: -101.7 and [b]: -101.8 kJ mol^{-1}) are an exception to all calculated E_i values. This is probably a consequence of the disruption by the presence of the arylisouronium of the intramolecular HBs' net that exists in the ATP molecule (see Figure S1, bottom right). When the interaction occurs by the 'right' side of the ATP molecule, allowing its natural intramolecular HBs' net, the E_i values obtained for both phosphates β and γ are stronger than for the α-phosphate. For complexes type **I** the most stable configuration is γ-D[*a*] in which the interaction occurs with the end phosphate of the ATP molecule by the bottom side. Moreover, β-R complexes **I** are more stable than the corresponding α-R systems because, even though they establish similar parallel HBs (see Figure S2), the β-R complexes do not disrupt the intramolecular HBs' net in ATP.

The E_i values calculated for the 4-phenyloxyphenyl-*O*-isouronium···ATP complexes are larger than those previously reported by our group for 4-phenyloxyphenyl-*N*-guanidinium···ATP interactions (Table S1).[S1] However, an exception to this trend is found in complexes type **II** which show a slightly stronger E_i for the arylguanidinum···ATP complex than for the isouronium analogue. This is due to the extra H atom of the guanidinium cation which may interact with the phosphate groups (Figure S2). Since the larger the number of interactions, the larger the Ei values, it is clear from Table S1 that complexes type **II** (multiple simultaneous interactions with different phosphates) are more stable than similar complexes type **I** (only one interaction with the phosphates).

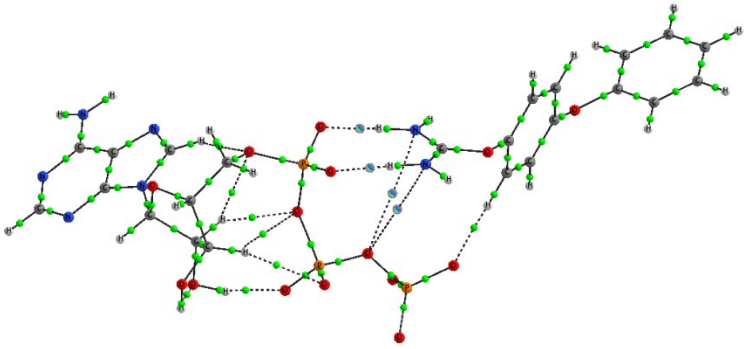

Iα-R[a]

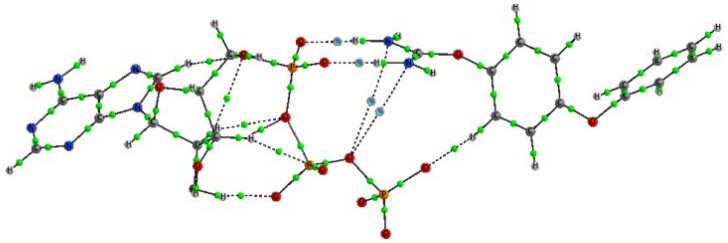

Iα-R[b]

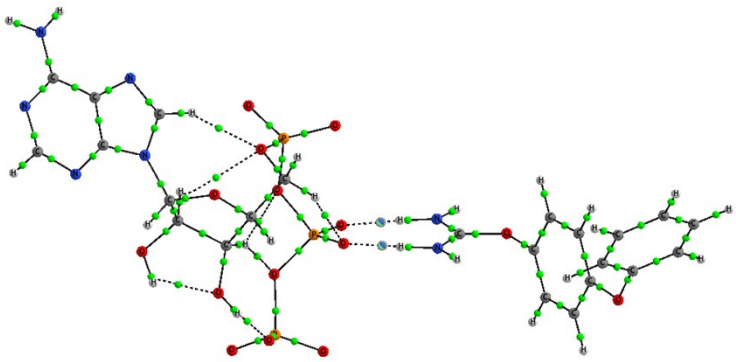

Iβ-R[a]

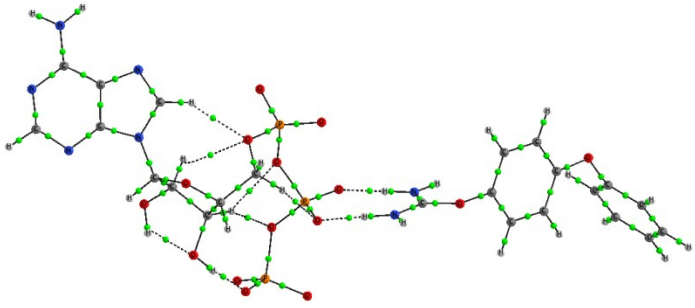

Iβ-R[b]

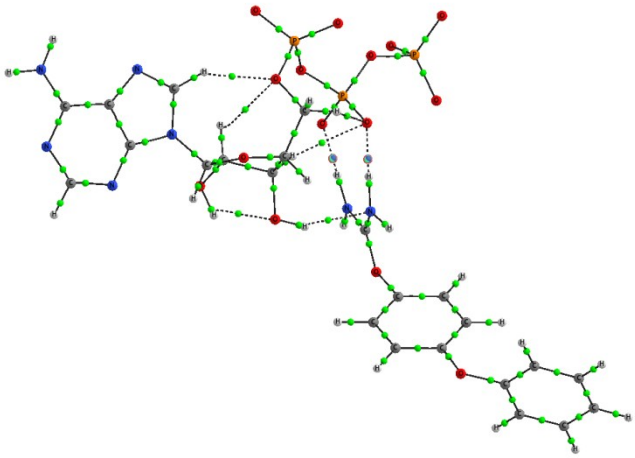

Iβ-L[a]

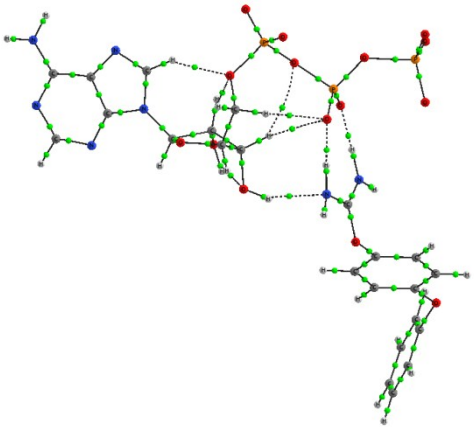

Iβ-L[b]

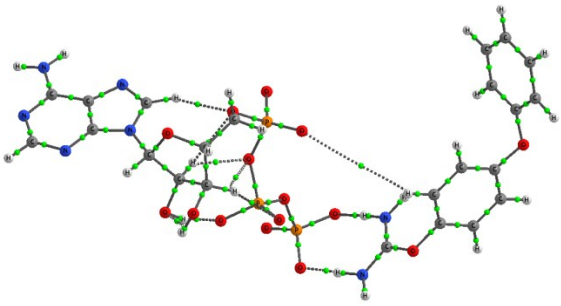

Iγ-R[a]

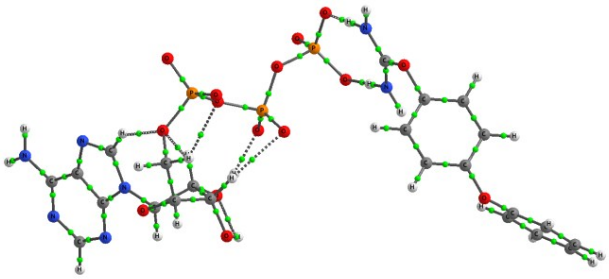

Iγ-R[b]

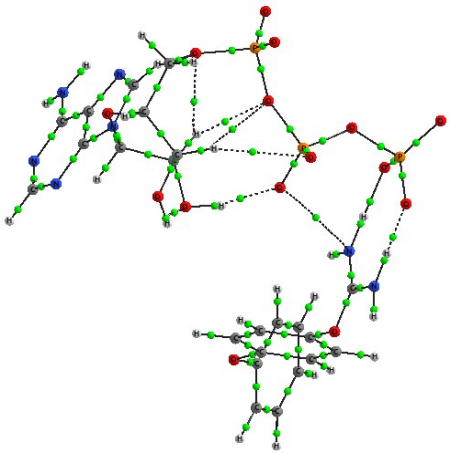

Iγ-L[a]

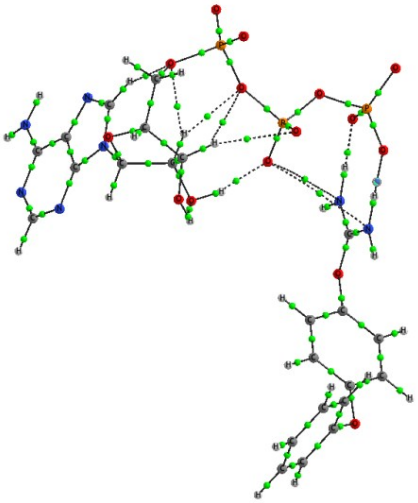

Iγ-L[b]

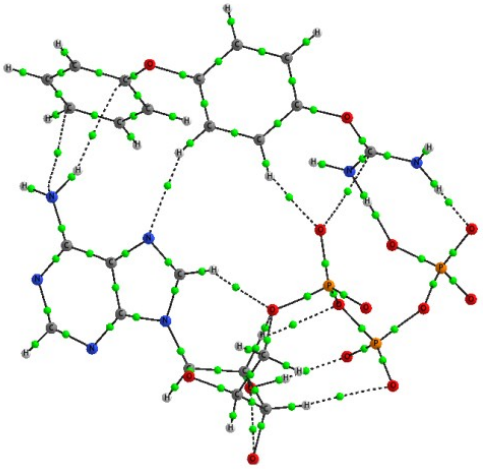

Iγ-D[a]

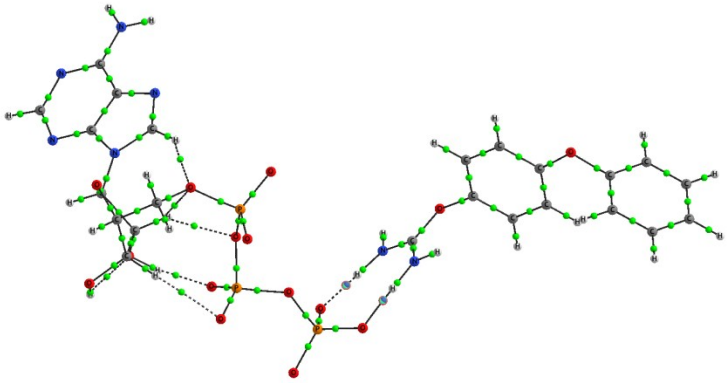

Iγ-D[b]

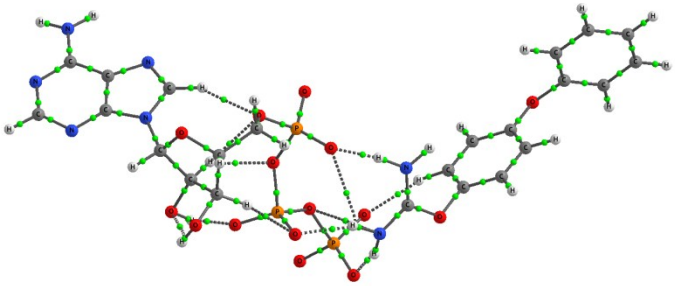

IIγ-R[a]

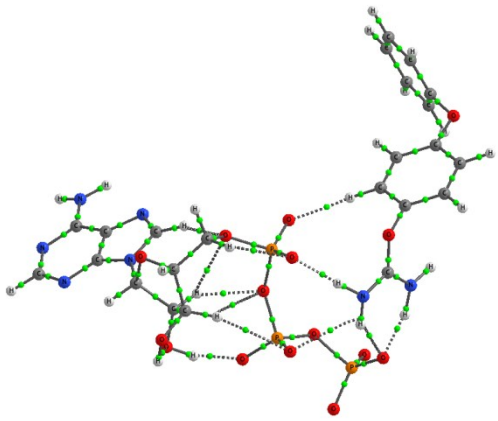

IIγ-R[b]

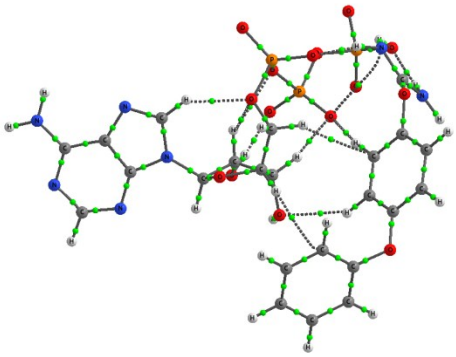

IIγ-L[a]

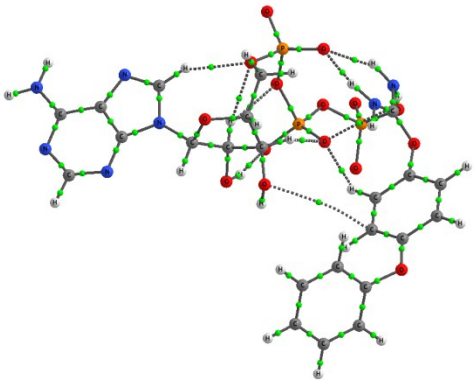

IIγ-L[b]

Figure S2: Molecular graphs corresponding to complexes **I** and **II** between arylisouronium and the phosphates α, β and γ of the ATP molecule. Green dots correspond to bond critical points (BCP) as per the Atoms in Molecules theory.

All the interactions established within the 4-phenyloxyphenyl-*O*-isouronium-ATP complexes (**I** and **II**) were characterized by analysing their electron density topology using the Atoms in Molecules (AIM) theory [ref. 29 in the manuscript]. Thus, the characteristics of the Bond

Critical Points (BCPs) found between the interacting moieties, i.e. electron density at the BCP (ρBCP) and Laplacian of the electron density at the BCP (∇^2ρBCP), were calculated and are presented in Tables S2 and S3. The ρBCP values and positive Laplacians, indicate that all the interactions established within complexes type **I** and **II** are of non-covalent nature and can be classified as HBs. The AIM molecular graphs corresponding to all complexes type **I** and **II** interacting with the α-, β- and γ-phosphates are exhibited in Figure S2.

Table S2 shows that in the interactions in complexes type **I** (parallel HBs) the ρBCP values for the isouronium-phosphate interactions follow the order γ > β > α, which is the same order observed for the E_i values. Moreover, similar to the calculated E_i, the ρBCP for the 4-phenyloxyphenyl-*O*-isouronium complexes are larger than the corresponding ρBCP for the arylguanidinium ones. An exponential correlation between the value of the ρBCP and the corresponding interatomic distance has been found (Figure S3) indicating how the ρBCP decreases with the increase of the interatomic distance for complexes type **I**.

Analysis of all complexes type **II** (Table S3) indicates multiple interactions between the arylisouronium and the ATP phosphates as for example complex **II**γ-R[a] in which the isouronium moiety forms HBs with the three ATP phosphates (see Figure S2). As mentioned, these complexes type **II** present larger E_i than complexes type **I** because of the multiple isouronium-phosphates HBs formed (Table S1); however, the corresponding ρBCP values are smaller because these multiple HBs are bifurcated, which are less stable than the parallel interactions found in complexes type **I**.[S3]

In order to obtain a better insight into the electron density changes upon complexation, electron density shift maps (EDS) were obtained. Only one example for the complexes between α, β and γ phosphates and the arylisouronium has been studied. Therefore, EDS were obtained for **I**α-R[a], **I**β-R[a] and **I**γ-L[b] following the procedure previously reported (ref. 42 in manuscript) and are shown in Figure S4. The density shift pattern shown in Figure S4 indicates that a decrease of the electron density occurs around the H attached to the HB donor as revealed by a light blue region. Also an increase in the intermolecular density (purple region) is observed in the area between that H atom and the HB acceptors (N or O).

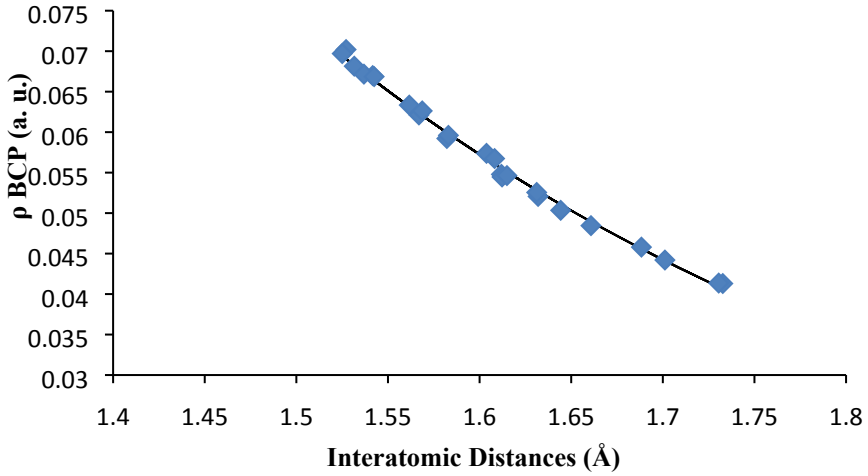

Figure S3: Relationship between the interatomic distance (Å) and the value of the electron density at BCP (a.u.) for H···X (X=O, N) interactions for complexes **I**.

Table S2. Electron density at the bond critical points (ρBCP, a.u.), the Laplacian of that electron density (∇^2ρBCP, a.u.) and interatomic distances (Å) calculated at ωB97XD/6-31+G(d,p) and PCM-water computational level for all complexes **I**.

	O1···H2N2			**O2···H3N3**		
Complex	ρBCP	∇^2ρBCP	Å	ρBCP	∇^2ρBCP	Å
Iα-R[a]	0.046	0.133	1.688	0.041	0.121	1.730
Iα-R[b]	0.041	0.120	1.733	0.044	0.130	1.701
Iβ-R[a]	0.048	0.141	1.661	0.054	0.155	1.612
Iβ-R[b]	0.052	0.148	1.632	0.050	0.147	1.644
Iβ-L[a]	0.055	0.154	1.612	0.054	0.152	1.615
Iβ-L[b]	0.059	0.159	1.582	0.052	0.149	1.631
Iγ-R[a]	0.070	0.160	1.527	0.057	0.151	1.604
Iγ-R[b]	0.067	0.160	1.542	0.063	0.158	1.569
Iγ-L[a]	0.068	0.162	1.532	0.060	0.157	1.583
Iγ-L[b]	0.062	0.160	1.567	0.067	0.163	1.537
Iγ-D[a]	0.070	0.164	1.525	0.057	0.151	1.608
Iγ-D[b]	0.063	0.160	1.562	0.067	0.160	1.542

Table S3. Electron density at the bond critical points (ρBCP, a.u.), the Laplacian of that electron density (∇^2ρBCP, a.u.) calculated at ωB97XD/6-31+G(d,p) and PCM-water computational level for all complexes **II**.

	PαO···HN	**PαO···HN**	**PβO···N**	**PβO···N**	**PγO···HN**	**PγO···HN**	**PO···HC**
Complex	**ρBCP** ∇^2**ρBCP**	**ρBCP** ∇^2**ρBCP**	**ρBCP** ∇^2**ρBCP**	**ρBCP** ∇^2**ρBCP**	**ρBCP** ∇^2**ρBCP**	**ρBCP** ∇^2**ρBCP**	**ρBCP** ∇^2**ρBCP**
IIγ-L[b]	0.0359	0.0227	-	-	0.0597	-	0.0174
	0.1138	0.0669	-	-	0.1615	-	0.0573
IIγ-R[a]	0.0469	0.0057	0.0302	0.0078	0.0542	-	0.0167
	0.1446	0.0241	0.0886	0.0267	0.1488	-	0.0473
IIγ-L[a]	0.0400	-	-	-	0.0367	0.1054	0.0239
	0.1267	-	-	-	0.1054	0.1097	0.0764
IIγ-R[b]	0.0378	-	0.0094	-	0.0244	0.0569	0.0154
	0.1133	-	0.0353	-	0.0680	0.1553	0.0454

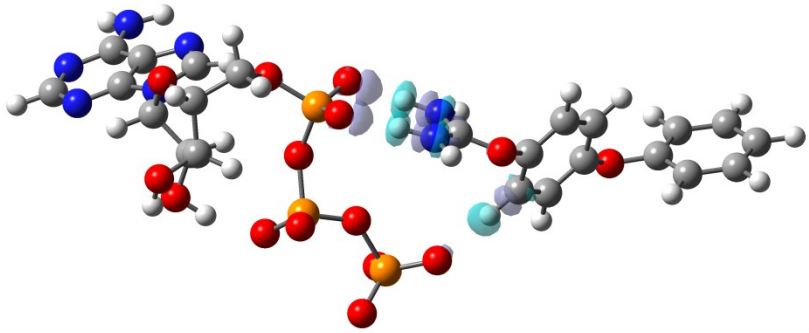

Iα-R[a]

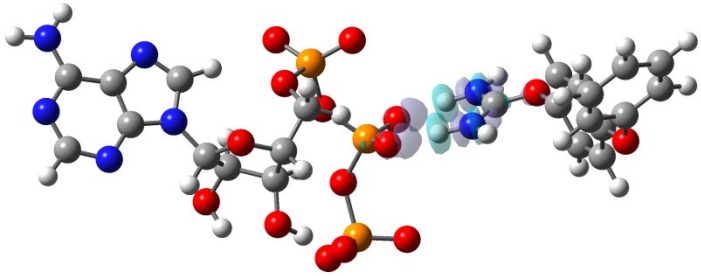

Iβ-R[a]

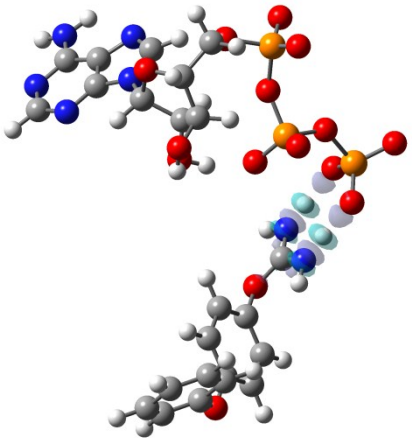

Iγ-L[b]

Figure S4: Electron Density Shifts at 0.003 a.u. calculated for complexes **I- α, β** and **γ** at MP2/6-31+G(d,p) computational level. **Purple** and **light blue** areas represent positive (increase) and negative (decrease) electron density regions respectively.

2. Chemistry

2.1. General procedure: Method A

Mercury (II) chloride ($HgCl_2$) (1.04 eq.) was added over a 0.19 M solution of the corresponding amine (1 eq.), the corresponding thiourea (1.04 eq.) and triethylamine (Et_3N) (3.5 eq.) in dichloromethane (CH_2Cl_2) at 0 °C. The resulting mixture was stirred at 0 °C for 1 h and then at room temperature for further 2 - 4 hours or overnight depends on the reactivity of the substrates and possible generation of side products (reaction progress adjudged by TLC). The crude was then diluted with with EtOAc and filtered through a pad of Celite® in order to remove the mercury sulfide precipitate formed. The filter cake was rinsed with EtOAc. The organic phase was extracted with water, washed with brine, dried over anhydrous $MgSO_4$, and concentrated under vacuum to give a residue that was purified by flash chromatography on silica gel as specified.

2.2. General procedure: Method B

The appropriate benzoic acid derivative (1.2 eq.) was placed under nitrogen atmosphere and dissolved in a 0.3 M solution of dry dichloromethane (CH_2Cl_2). Oxalyl chloride (2 eq.) was added, followed by dimethylformamide (DMF) (3 drops approx.). The solution was stirred overnight. Any remaining oxalyl chloride and DMF was removed under vacuum to obtain a yellow residue that was dissolved in CH_2Cl_2 (0.6 M) and cooled to 0 ºC. Corresponding aniline (1 eq.) and triethylamine (Et_3N) (2.4 eq.) was also dissolved in CH_2Cl_2 and added dropwise to the cooled solution. After 2 h the solution was warmed to room temperature. The organic layer was extracted using water, washed with brine, dried over $MgSO_4$ and concentrated under vacuum to give a residue. It was purified by flash chromatography (eluting with a gradient of hexane:EtOAc) to yield final compound.

2.3. Preparation of intermediates

It has been previously observed in Rozas' group that the ^1H and ^{13}C NMR spectra of different *N*,*N'*-bis-aryl-*N''*-Boc protected guanidines were always characterised by broad, poorly resolved signals. This phenomenon was attributed to the interconversion between different tautomers, which are induced by the sterically-congested environment surrounding the central guanidine moiety Hence, for compound **12**, **13** and **15**, aromatic protons and carbons, quaternary carbons and fluorine peaks could not be fully assigned and characterised because the peaks were very broad.[S4]

2-(4-Iodophenoxy)tetrahydro-2*H*-pyrane (6)[S5]

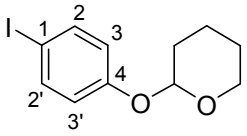

To a solution of 4-iodophenol (1.10 g, 5 mmol) and pyridinium *p*-toluenesulfonate (PPTS) (126 mg, 0.5 mmol) in dry CH_2Cl_2 (25 mL) was added 3,4- dihydro-2H-pyran (0.7 mL, 7.5 mmol).

The resultant mixture was stirred for 2.5 h at room temperature. The reaction mixture was diluted with diethyl ether and washed once with saturated brine. The organic layer was dried over anhydrous Na_2SO_4, filtered, and concentrated under reduced pressure. Purification by flash column chromatography over silica gel (10% EtOAc in hexane) gave the product 8 as a white solid (1.2 g, 82%). **Mp**: 63-64°C (lit. 64-65 °C).

δ_H (400 MHz, $CDCl_3$): 1.56 – 1.73 (m, 3H, CH_2), 1.82 – 1.86 (m, 2H, CH_2), 1.92 – 2.03 (m, 1H, CH_2), 3.55 – 3.61 (m, 1H, CH_2), 3.82 – 3.88 (m, 1H, CH_2), 5.36 (t, *J* = 3.2 Hz, 1H, CH), 6.82 (dd, *J* = 8.4, 3.7 Hz, 2H, H-3 and H-3'), 7.54 (dd, *J* = 8.4, 3.7 Hz, 2H, H-2 and H-2').

3-{4-[(Tetrahydro-2*H*-pyran-2-yl)oxy]phenoxy}aniline (8)[S6]

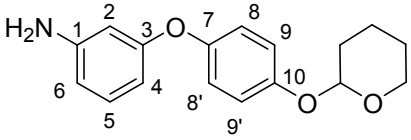

An oven-dried screw cap test tube was charged with a magnetic stirbar, copper(I) iodide (20.8 mg, 0.11 mmol, 5 mol%), 2-picolinic acid (26.8 mg, 0.22 mmol, 10 mol%), aryl iodide **6** (661.8 mg, 2.18 mmol), 3-aminophenol (285.9 mg, 2.62 mmol) and K_3PO_4 (926 mg, 4.36 mmol). The tube was then evacuated and back-filled with argon. The evacuation/backfill sequence was repeated two additional times. Under a counterflow of argon dimethylsulfoxide (4.0 mL) was added by syringe. The tube was placed in a preheated oil bath at 80 ºC and the reaction mixture was stirred vigorously for 24 h. The reaction mixture was cooled to room temperature and diluted with EtOAc and H_2O. The organic layer was separated and the aqueous layer was extracted twice more with EtOAc. Combined organic layers were dried over Na_2SO_4 and the filtrate was concentrated and the resulting residue was purified via silica-gel chromatography (gradient 3:1 hexane- EtOAc) to give **8** (534 mg, 86%) as a yellow liquid.

δ_H (400 MHz, $CDCl_3$): 1.58 – 1.73 (m, 3H, CH_2), 1.84 – 1.88 (m, 2H, CH_2), 1.96 – 2.04 (m, 1H, CH_2), 3.59 – 3.64 (m, 1H, CH_2),3.90 – 3.98 (m, 1H, CH_2), 5.35 (t, *J* = 3.4 Hz, 1H, CH), 6.33 (t, *J* = 2.2 Hz, 1H, H-2), 6.38 (dd, *J* = 8.2, 2.3 Hz, 1H, H-4), 6.42 (dd, *J* = 7.3, 2.1 Hz, 1H, H-6), 6.96 (d, *J* = 9.2 Hz, 2H, H-8 and H-8' or H-9 and H-9'), 7.03 (d, *J* = 9.1 Hz, 2H, H-9 and H-9' or H-8 and H-8'), 7.07 (t, *J* = 8.1 Hz, 1H, H-5).

δ_C (150 MHz, $CDCl_3$): 19.0 (CH_2), 25.4 (CH_2), 30.6 (CH_2), 62.3 (CH_2), 97.4 (CH), 105.1 (CH Ar, C-2), 108.6 (CH Ar, C-4), 110.0 (CH Ar, C-6), 117.8 (2 CH Ar, C-8 and C-8' or C-9 and C-9'), 121.0 (2 CH Ar, C-8 and C-8' or C-9 and C-9'), 130.4 (CH Ar, C-5), 147.0 (qC), 150.9 (qC), 153.4 (qC), 159.7 (qC).

HRMS (m/z ESI^+): Found 286.1454 (M^+ + H. $C_{17}H_{20}NO_3$, Requires: 286.1443).

ν_{max} (ATR)/cm^{-1}: 3331 (NH), 2944 (CH), 2872 (CH), 1654, 1601, 1499, 1486, 1242, 1197 (C-O), 1180, 1034, 961, 835, 776, 660, 685.

1-(4-chloro-3-trifluoromethylphenyl)-3-{3-[4-(tetrahydro-2*H*-pyran-2-yl)oxyphenoxy] phenyl}-2-(*tert*-butoxycarbonyl)guanidine (12)

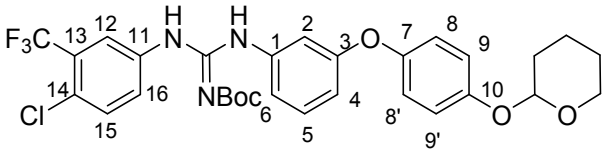

Following Method A, $HgCl_2$ (226 mg, 0.83 mmol) was added to a solution of **8** (228 mg, 0.80 mmol), *N*-(4-chloro-3-trifluoromethylphenyl)-*N'*-Boc-thiourea **11** (294 mg, 0.83 mmol) and Et_3N (0.39 mL, 2.80 mmol) in CH_2Cl_2 (5 mL). The reaction was stirred overnight at room temperature and then diluted with EtOAc and filtered through Celite® and washed with EtOAc. Usual work-up, followed by purification of the product by silica gel chromatography eluting with a gradient of 100% hexane to 90:10 hexane:Et_2O respectively to afford the title product as a white solid (282 mg, 58%). **Mp**: 48-51 °C

δ_H (400 MHz, $CDCl_3$): 1.72 (s, 9H, $(CH_3)_3$), 1.82 – 1.96 (m, 3H, CH_2), 2.08 – 2.10 (m, 2H, CH_2), 2.19 – 2.24 (m, 1H, CH_2), 3.82 – 3.86 (m, 1H, CH_2), 4.13 – 4.19 (m, 1H, CH_2), 5.58 (s, 1H, CH), 6.74 – 6.99 (m, 4H, CH Ar), 7.20 – 7.28 (m, 4H, CH Ar), 7.48 – 7.50 (m, 2H, CH Ar), 7.62 – 7.64 (m, 1H, CH Ar), 8.17 (s, 1H, NH), 10.04 (s, 1H, NH).

δ_C (100 MHz, $CDCl_3$): 19.0 (CH_2), 25.3 (CH_2), 28.2 ($(CH_3)_3$), 30.5 (CH_2), 62.2 (CH_2), 83.9 (qC, $\underline{C}(CH_3)_3$), 97.1 (CH), 111.6, 112.8, 116.4, 117.8, 118.8, 120.9, 121.5, 122.1, 123.9, 124.2, 126.8, 129.9, 130.8, 131.8, 132.5, 137.9, 139.9, 150.6, 153.1, 153.6, 171.2.

Note: Aromatic protons and carbons, quaternary carbons and fluorine peaks could not be fully assigned and characterised because the peaks were very broad.

HRMS (m/z ESI^-): Found: 604.1823 (M^- - H. $C_{30}H_{30}N_3O_5ClF_3$ Requires: 604.1826).

ν_{max} (ATR)/cm^{-1}: 3410 (NH),2916 (CH), 2848 (CH), 1722 (C=O), 1664, 1590, 1556, 1500 (C=N), 1478, 1465, 1322, 1238, 1209, 1198, 1198, 1141 (CF_3), 1110 (C-Cl), 906, 731, 666.

1-(4-chloro-3-trifluoromethylphenyl)-3-[3-(4-hydroxyphenoxy)phenyl]-2-(*tert*-butoxycarbonyl)guanidine (13)

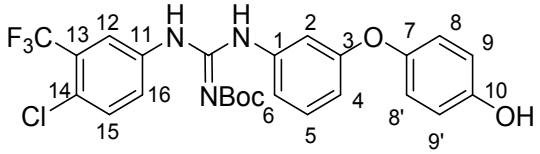

A mixture of **12** (244 mg, 0.40 mmol), methanol (4 mL) and montmorillonite KSF (230 mg) was stirred at 50 °C for 1h. The progress of the reaction was monitored by TLC. After completion of the reaction, the catalyst was removed by filtration and washed with EtOAc. Evaporation of the solvent gave the corresponding crude product that was further purified by

silica gel chromatography eluting with a gradient of 100% hexane to 80:20 hexane:EtOAc respectively, to afford the title product as a white solid (135 mg, 65%). **Mp**: 52-55 °C

δ_H (400 MHz, $CDCl_3$): 1.48 (s, 9H, $(CH_3)_3$), 6.41 – 6.73 (m , 3H, CHAr), 6.79 – 6.81 (m, 3H, CHAr), 6.91 – 7.00 (m, 3H, CHAr), 7.15 – 7.24 (m, 1H, CHAr), 7.38 – 7.40 (m, 1H, CHAr), 7.90 (bs), 9.81 (bs).

δ_C (100 MHz, $CDCl_3$): 28.2 ($(CH_3)_3$), 84.1 (qC, $\underline{C}(CH_3)_3$), 111.5, 112.6, 112.7, 116.5, 118.7, 119.2, 121.4, 124.2, 126.9, 128.9, 130.2, 130.8, 131.9, 132.2, 137.7, 140.3, 149.8, 152.3, 153.1, 153.2, 160.1.

Note: Aromatic protons and carbons, quaternary carbons and fluorine peaks could not be fully assigned and characterised because the peaks were very broad.

HRMS (m/z ESI^-): Found: 520.1246 (M^- - H. $C_{25}H_{22}N_3O_4ClF_3$ Requires: 520.1251).

ν_{max} (ATR)/cm^{-1}: 3407 (NH), 3295 (OH), 2983, 1722 (C=O), 1658, 1589, 1556, 1505, 1461, 1203, 1140 (CF_3), 1092 (C-Cl), 835, 772.

N,N'-di(*tert*-butoxycarbonyl)-4-{3-[*N*-(*tert*-butoxycarbonyl)-3-(4-chloro-3-trifluoromethylphenyl)guanidino] phenoxy}phenyl carbamimidate (15)

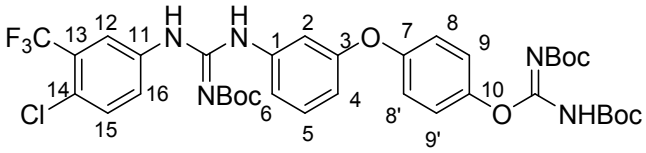

Following a modification of Method A, $HgCl_2$ (114 mg, 0.42 mmol) was added over a solution of **13** (207 mg, 0.40 mmol), *N,N'*-bis-(*tert*-butoxycarbonyl)-*S*-methylisothiourea **14** (122 mg, 0.42 mmol) and Et_3N (0.20 mL, 1.4 mmol) in CH_2Cl_2 (4 mL) at 0 °C. The resulting mixture was stirred at 0 °C for 1 h and overnight at room temperature. Usual work-up, followed by purification of the crude product by silica gel chromatography eluting with a gradient of 100% hexane to 90:10 hexane:EtOAc respectively to afford the title product as a white-yellow solid (168 mg, 55%). **Mp**: 63-65 °C.

δ_H (400 MHz, $CDCl_3$): 1.33 – 1.65 (m, 27H, $(CH_3)_3$), 6.56 – 6.75 (m, 3H, CH Ar), 6.88 – 7.02 (m, 3H, CH Ar), 7.14 – 7.23 (m, 2H, CH Ar), 7.39 – 7.49 (m, 2H, CH Ar), 7.84 – 7.92 (m, 1H, CH Ar), 9.82 (bs, NH), 10.64 (bs, NH), 11.61 (bs, NH).

δ_C (100 MHz, $CDCl_3$): 28.1 ($(CH_3)_3$), 28.2 ($(CH_3)_3$), 84.0 (qC, $\underline{C}(CH_3)_3$), 112.7, 113.6, 116.5, 117.3, 119.0, 120.0, 121.3, 121.5, 122.1, 123.1, 124.2, 126.9, 130.1, 131.0, 131.8, 132.3, 132.8, 137.8, 140.1, 146.9, 148.0, 153.1, 154.5, 158.9.

Note: Aromatic protons and carbons, quaternary carbons and fluorine peaks could not be fully assigned and characterised because the peaks were very broad.

HRMS (m/z ESI$^+$): Found: 764.2676 (M^+ + H. $C_{36}H_{42}N_5O_8ClF_3$ Requires: 764.2674).

ν_{max} (ATR)/cm^{-1}: 3415 (NH), 3268 (NH), 2981, 2933, 1769 (C=O), 1722 (C=O), 1659 (C=N), 1565 (C=N), 1410, 1297, 1238, 1132 (CF_3), 1088 (C-Cl), 957, 829 , 770.

4'-[2,3-Di-(tert-butoxycarbonyl)guanidino]-3-[4-chloro-3-(trifluoromethyl)benzamido] diphenylether (19)

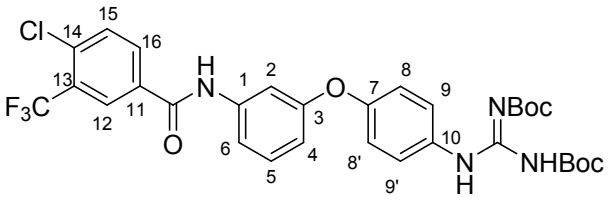

Following Method B, to a solution of 4-chloro-3-trifluoromethylbenzoic acid (183 mg, 0.82 mmol) in CH_2Cl_2 (3 mL), oxalyl chloride (0.1 mL, 1.36 mmol) and DMF (3 drops) were added and the reaction was stirred overnight. Any remaining oxalyl chloride and DMF were removed under vacuum to obtain **18** as a yellow residue that was dissolved in CH_2Cl_2 and cooled to 0 °C. Compound **17** (300 mg, 0.68 mmol) dissolved in CH_2Cl_2 (1.13 mL) and Et_3N (0.23 mL, 1.63 mmol) was added dropwise and, after 12 h, workup and silica gel chromatography afforded **19** (225 mg, 51%) as a yellow oil.

δ_H (600 MHz, $CDCl_3$): 1.55 (s, 9H, $(CH_3)_3$), 1.57 (s, 9H, $(CH_3)_3$), 6.81 (dd, *J* = 8.2, 1.7 Hz, 1H, H-4), 6.86 (d, *J* = 8.8 Hz, 2H, H-8 and H-8' or H-9 and H-9'), 6.96 (s, 1H, H-2), 7.28 (t, *J* = 8.2 Hz, 1H, H-5), 7.36 (d, *J* = 8.8 Hz, 2H, H-8 and H-8' or H-9 and H-9'), 7.55 - 7.58 (m, 2H, H-15, H-6), 7.98 (dd, *J* = 8.3, 1.8 Hz, H-16), 8.25 (d, *J* = 1.6 Hz, 1H, H-12), 8.74 (s, 1H, NH), 10.19 (s, 1H, NH), 11.62 (s, 1H, NH).

δ_C (150 MHz, $CDCl_3$): 28.2 (2$(CH_3)_3$), 84.4 (qC, 2 C$(CH_3)_3$), 109.9 (CH Ar, C-2), 114.9 (CH Ar, C-4), 115.2 (CH Ar, C-6), 120.6 (2 CH Ar, C-8 and C-8' or C-9 and C-9'), 122.7 (d, *J* = 273.9 Hz, qCF_3), 124.3(qC), 125.1 (2 CH Ar, C-8 and C-8' or C-9 and C-9'), 127.1 (m, CH Ar, C-12), 130.4 (CH Ar, C-5), 131.91 (CH Ar, C-15), 131.95 (CH Ar, C-16), 132.0 (qC), 133.7 (qC), 136.0 (qC), 139.3 (qC), 153.3 (qC), 154.2 (qC), 154.3 (qC), 158.4 (qC), 158.5 (qC), 163.7 (qC).

HRMS (m/z ESI$^+$): Found 649.2042 (M^+ + H. $C_{31}H_{33}ClF_3N_4O_6$ Requires: 649.2041).

ν_{max} (ATR)/cm^{-1}: 3253 (NH), 2979, 2932, 1720 (C=O), 1648 (C=O), 1598, 1406, 1324, 1240, 1213, 1143 (CF_3), 1108 (C-Cl), 1056, 1035, 909, 730.

4-Chloro-3-trifluoromethyl-*N*-(3-{4-[(tetrahydro-2*H*-pyran-2-yl)oxy]phenoxy}phenyl) benzamide (20)

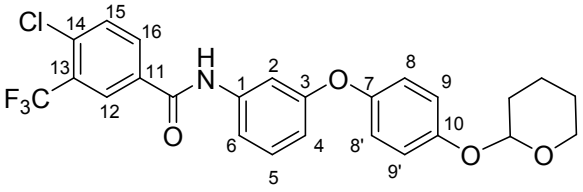

Following Method B, to a solution of 4-chloro-3-trifluoromethylbenzoic acid (321 mg, 1.43 mmol) in CH_2Cl_2 (5 mL), oxalyl chloride (0.1 mL, 2.4 mmol) and DMF (3 drops) were added and the reaction was stirred overnight. Any remaining oxalyl chloride and DMF were removed under vacuum to obtain **18** a yellow residue that was dissolved in CH_2Cl_2 and cooled to 0 °C. Compound **8** (340 mg, 1.20 mmol) dissolved in CH_2Cl_2 (2 mL) and Et_3N (0.40 mL, 2.88 mmol) were added dropwise, after 12 h, workup and silica gel chromatography afforded **20** (253 mg, 43%) as a white gum.

δ_H (400 MHz, $CDCl_3$): 1.64 – 1.70 (m, 3H, CH_2), 1.84 – 1.87 (m, 2H, CH_2), 1.95 – 2.00 (m, 1H, CH_2), 3.58 – 3.63 (m, 1H, CH_2), 3.90 – 3.96 (m, 1H, CH_2), 5.33 (t, *J* = 3.3 Hz, 1H, CH), 6.77 (dd, *J* = 8.1, 1.9 Hz, 1H, H-4), 6.95 (d, *J* = 9.1 Hz, 2H, H-8 and H-8' or H-9 and H-9'), 7.00 (d, *J* = 9.1 Hz, 2H, H-8 and H-8' or H-9 and H-9'), 7.14 (s, 1H, H-2), 7.27 (t, *J* = 8.1 Hz, 1H, H-5), 7.37 (d, *J* = 8.2 Hz, 1H, H-6), 7.59 (d, *J* = 8.3 Hz, 1H, H-15), 7.94 (dd, *J* = 8.3, 1.9 Hz, 1H, H-16), 7.99 (bs, NH), 8.16 (d, *J* = 1.5 Hz, 1H, H-12).

δ_C (100 MHz,$CDCl_3$): 21.2 (CH_2), 25.3 (CH_2), 30.6 (CH_2), 62.5 (CH_2), 64.0 (CH_2), 97.2 (CH), 109.7 (CH Ar, C-2), 114.6 (CH Ar, C-6), 116.6 (CH Ar, C-4), 117.9 (2 CH Ar, C-8 and C-8' or C-9 and C-9'), 121.1 (2 CH Ar, C-8 and C-8' or C-9 and C-9'), 121.5 (qC), 121.54 (d, *J* = 273.8 Hz, qCF_3), 126.6 (m, CH Ar, C-12), 129.1 (d, *J* = 21.9 Hz, qC, C-13), 130.3 (CH Ar, C-5), 131.6 (CH Ar, C-16), 132.1 (CH Ar, C-15), 133.7 (qC), 138.7 (qC), 150.5 (qC), 153.7 (qC), 159.3 (qC), 163.6 (qC).

HRMS (m/z ESI$^-$): Found 490.1032 (M^- - H, $C_{25}H_{20}NO_4ClF_3$ Requires: 490.1033).

ν_{max} (ATR)/cm^{-1}: 3310 (NH), 2945 (CH), 2873 (CH), 1738, 1652, 1601 (C=O), 1545, 1499, 1485, 1209, 1198 (CF_3), 1109 (C-Cl), 963, 919, 838, 871, 778 (C-Cl), 685, 660.

4-Chloro-3-trifluoromethyl-*N*-[3-(4-hydroxyphenoxy)phenyl]benzamide (21)

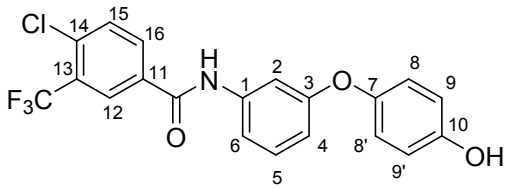

A mixture of **20** (240 mg, 0.49 mmol), methanol (4 mL) and montmorillonite KSF (250 mg) was stirred at 50 °C for 1h. The progress of the reaction was monitored by TLC. After

completion of the reaction, the catalyst was removed by filtration and washed with EtOAc. Evaporation of the solvent gave the corresponding crude product that was further purified by silica gel chromatography eluting with a gradient of 100% hexane to 90:10 hexane:EtOAc respectively to afford the title product as a white gum (148 mg, 74%).

δ_H (400 MHz, $CDCl_3$): 5.10 (bs, 1H, OH), 6.76 – 6.80 (m, 3H, H-8 and H-8' or H-9 and H-9' and H-4), 6.82 (d, *J* = 8.9 Hz, 2H, H-8 and H-8' or H-9 and H-9'), 6.95 (d, *J* = 8.9 Hz, 2H, H-8 and H-8' or H-9 and H-9'), 7.23 (bs, 1H, H-2), 7.28 – 7.31 (m, 2H, H-6 and H-5), 7.62 (d, *J* = 8.3 Hz, 1H, H-15), 7.85 (bs, 1H, NH), 7.95 (dd, *J* = 8.3, 2.1 Hz, 1H, H-16), 8.14 (d, *J* = 2.0 Hz, 1H, H-12).

δ_C (100 MHz, $CDCl_3$): 109.6 (CH Ar, C-2), 114.4 (CH Ar, C-4 or C-6), 114.5 (CH Ar, C-4 or C-6), 116.6 (2 CH Ar, C-8 and C-8' or C-9 and C-9'), 119.8 (d, *J* = 273.7 Hz, qCF_3),121.5 (2 CH Ar, C-8 and C-8' or C-9 and C-9'), 123.9 (qC),126.6 (m,CH Ar, C-12), 129.2 (d, *J* = 32.3 Hz, qC, C-13), 130.3 (CH Ar, C-5), 131.5 (CH Ar, C-16), 132.2 (CH Ar, C-15), 133.7 (qC), 138.6 (qC), 149.7 (qC), 152.4 (qC), 159.5 (qC), 163.6 (qC).

HRMS (m/z ESI^-): Found 406.0462 (M^- - H, $C_{20}H_{12}NO_3ClF_3$ Requires: 406.0458)

ν_{max} (ATR)/cm^{-1}: 3322 (OH), 2973 (CH), 1736 (C=O), 1659, 1602, 1505, 1486, 1444, 1243 (CF_3), 1142 (C-Cl), 1038 , 915, 843, 753, 701.

N,N'-di(*tert*-butoxycarbonyl)-4-{3-[4-chloro-3-(trifluoromethyl)benzamido]phenoxy} phenylcarbamimidate (22)

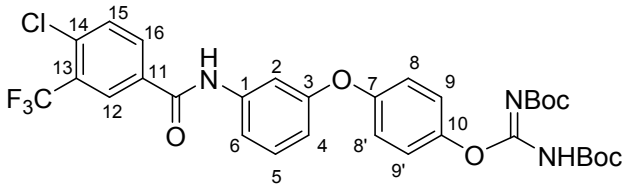

Following a modification of Method A, $HgCl_2$ (103 mg, 0.38 mmol) was added to a solution of starting phenol (150 mg, 0.37 mmol), *N,N'*-bis-(*tert*-butoxycarbonyl)-*S*-methylisothiourea **14** (111 mg, 0.38 mmol) and Et_3N (0.18 mL, 1.30 mmol) in CH_2Cl_2 (2 mL) at 0 °C. The resulting mixture was stirred at 0 °C for 1 h and overnight at room temperature. Usual work-up, followed by purification of the crude product by silica gel chromatography eluting with a gradient of 100% hexane to 90:10 hexane:EtOAc respectively to afford the title product (233 mg, 97%) as a yellow gum.

δ_H (400 MHz, $CDCl_3$): 1.43 (bs, 18H, 2$(CH_3)_3$)), 6.74 – 6.77 (m, 3H, H-8 and H-8' or H-9 and H-9' and H-4), 6.90 (d, *J* = 9.0 Hz, 2H, H-8 and H-8' or H-9 and H-9'), 6.98 (t, *J* = 2.0, 1H, H-2), 7.24 (t, *J* = 8.1 Hz, 1H, H-5), 7.50 (dd, *J* = 8.2, 1.0 Hz, H-6), 7.56 (d, *J* = 8.4 Hz, 1H, H-15), 8.03 (dd, *J* = 8.4, 1.9 Hz, 1H, H-16), 8.27 (d, *J* = 1.7 Hz, 1H, H-12), 9.08 (bs, 1H, NH).

δ_C (100 MHz, $CDCl_3$): 28.0 (s, 9H, $(CH_3)_3$), 28.1 (s, 9H, $(CH_3)_3$), 83.4 (qC, $\underline{C}(CH_3)_3$), 83.5 (qC, $\underline{C}(CH_3)_3$), 110.9 (CH Ar, C-2), 115.4 (CH Ar, C-4 or C-6), 115.9 (CH Ar, C-4 or C-6),

119.5 (2 CH Ar, C-8 and C-8’ or C-9 and C-9’), 122.7 (d, J = 273.7 Hz, qCF_3), 122.9 (2 CH Ar, C-8 and C-8’ or C-9 and C-9’), 126.8 (qC, C-14), 126.9 (q, J = 5.1 Hz, CH Ar, C-12), 128.5 (q, J = 31.9 Hz, qC, C-13), 130.3 (CH Ar, C-5), 131.0 (CH Ar, C-15), 132.5 (CH Ar, C-16), 133.6 (qC), 136.0(qC), 139.5 (qC), 146.3 (qC), 148.9 (qC), 154.9 (qC), 157.3 (qC), 159.1 (qC), 163.7 (qC).

HRMS (m/z ESI$^-$): Found 648.1721 (M^- - H, $C_{31}H_{30}N_3O_7ClF_3$, Requires: 648.1724)

ν_{max} (ATR)/cm^{-1}: 3412 (NH), 3314 (NH), 2981 (CH), 1769 (C=O), 1737, 1663, 1630, 1620, (C=N)1484, 1369, 1293, 1245, 1131 (CF_3), 1089 (C-Cl), 913, 874, 822, 752.

2.4. ^{1}H, ^{13}C, and ^{19}F NMR spectra and HPLC chromatogram of the final salts prepared

Compound 2:

^{1}H-NMR (CD_3OD)

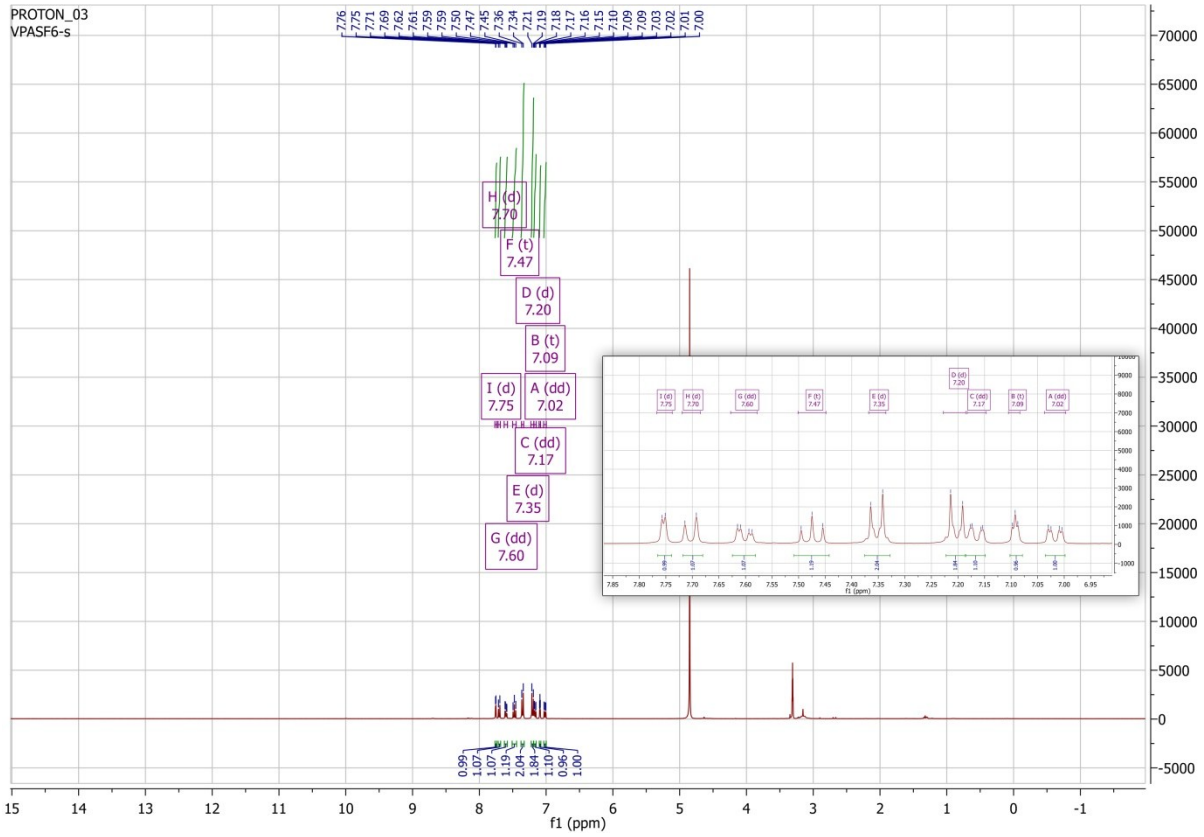

^{13}C-NMR (CD_3OD)

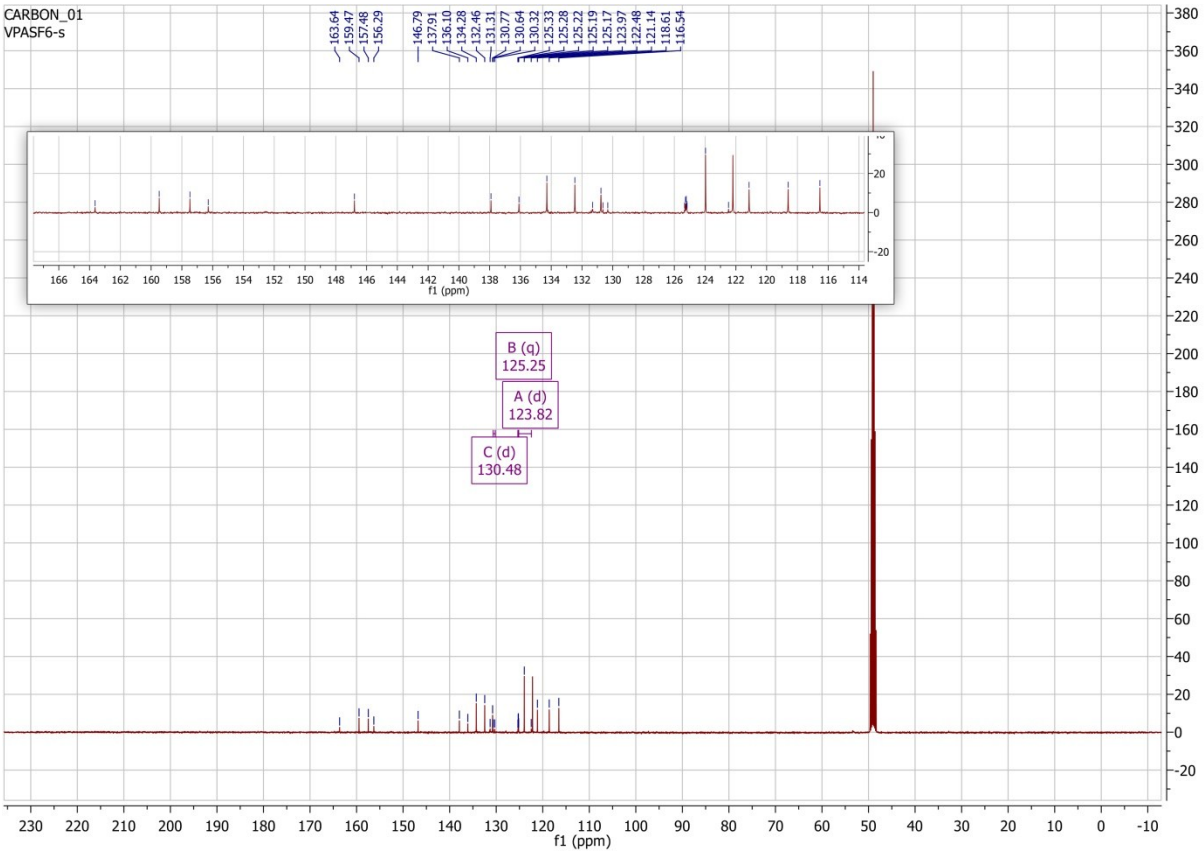

^{19}F-NMR (CD_3OD)

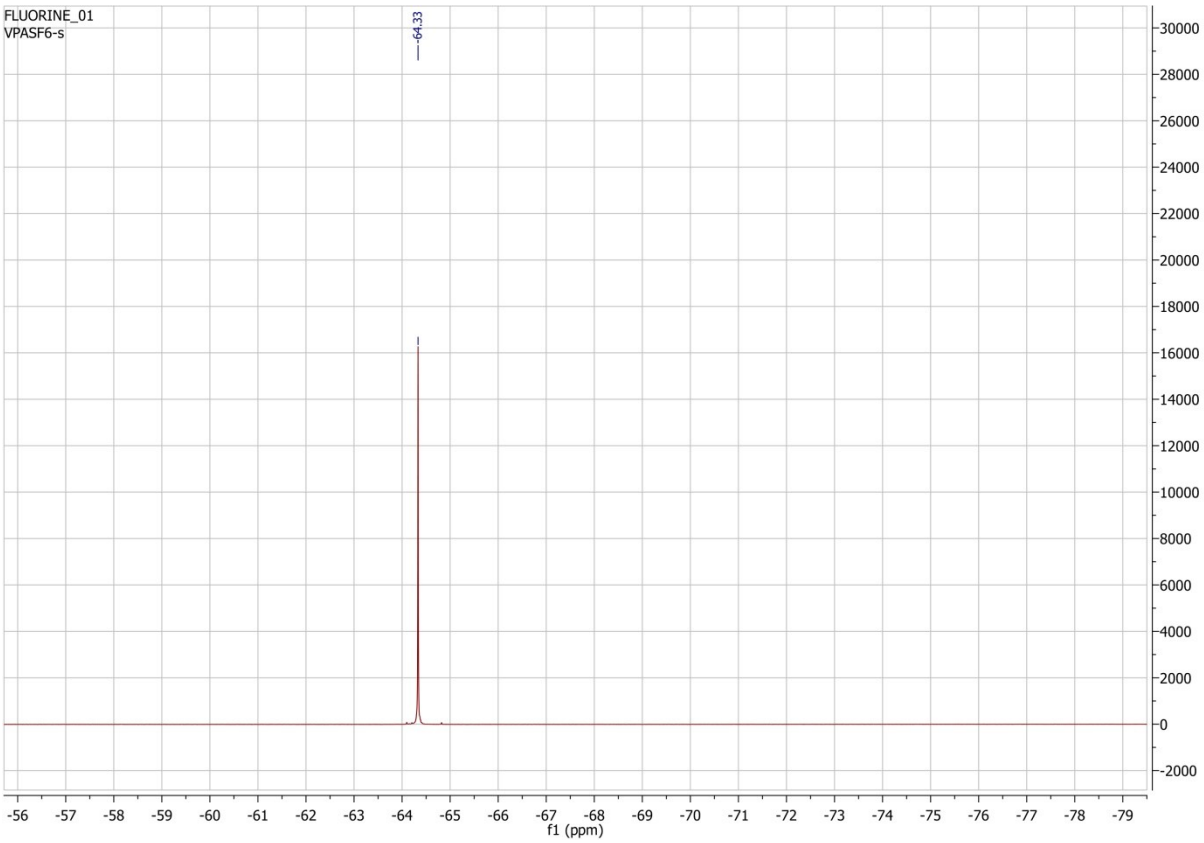

HPLC

Chromatogram : VPASF6-s_channel1

System : HPLC-PDA
Method : Gradient1
User : Daniel

Acquired : 27/09/2016 10:44:45
Processed : 27/09/2016 11:32:12
Printed : 27/09/2016 16:25:16

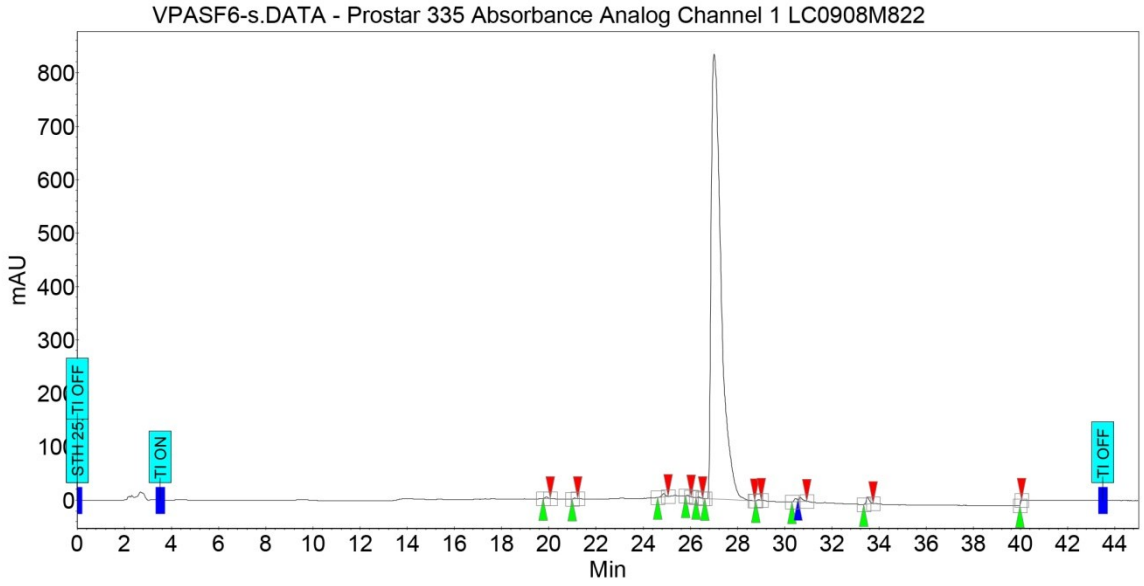

Peak results :

Index	Name	Time [Min]	Quantity [% Area]	Height [mAU]	Area [mAU.Min]	Area % [%]
1	UNKNOWN	19.89	0.11	3.4	0.4	0.106
2	UNKNOWN	21.09	0.05	1.9	0.2	0.046
3	UNKNOWN	24.87	0.23	5.9	1.0	0.232
4	UNKNOWN	25.89	0.05	1.9	0.2	0.049
5	UNKNOWN	26.36	0.06	1.9	0.2	0.059
6	UNKNOWN	27.01	98.43	833.2	405.4	98.430
7	UNKNOWN	28.89	0.04	1.9	0.2	0.045
8	UNKNOWN	30.47	0.21	6.1	0.9	0.208
9	UNKNOWN	30.67	0.30	7.3	1.2	0.300
10	UNKNOWN	33.52	0.46	12.6	1.9	0.458
11	UNKNOWN	40.00	0.07	8.3	0.3	0.067
Total			100.00	884.4	411.9	100.000

Compound 3:

^{1}H-NMR (CD_3OD)

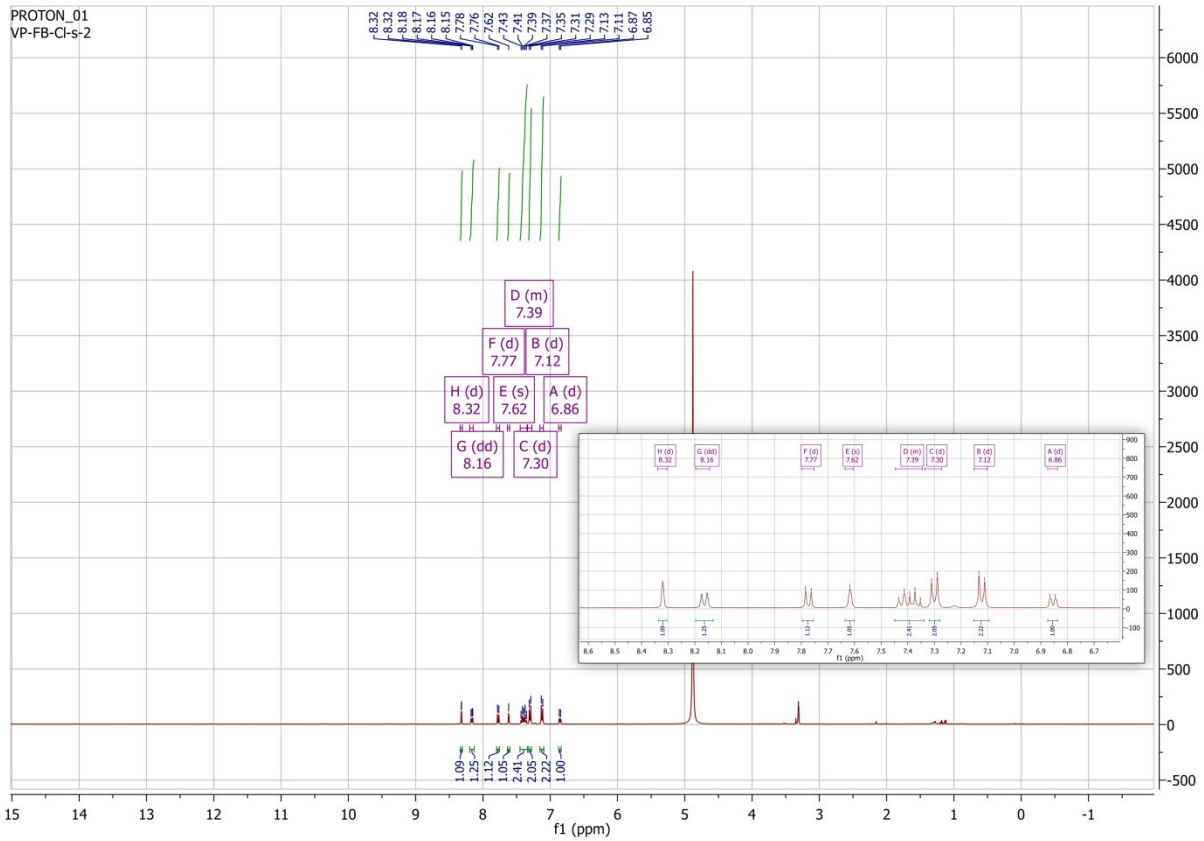

^{13}C-NMR (CD_3OD)

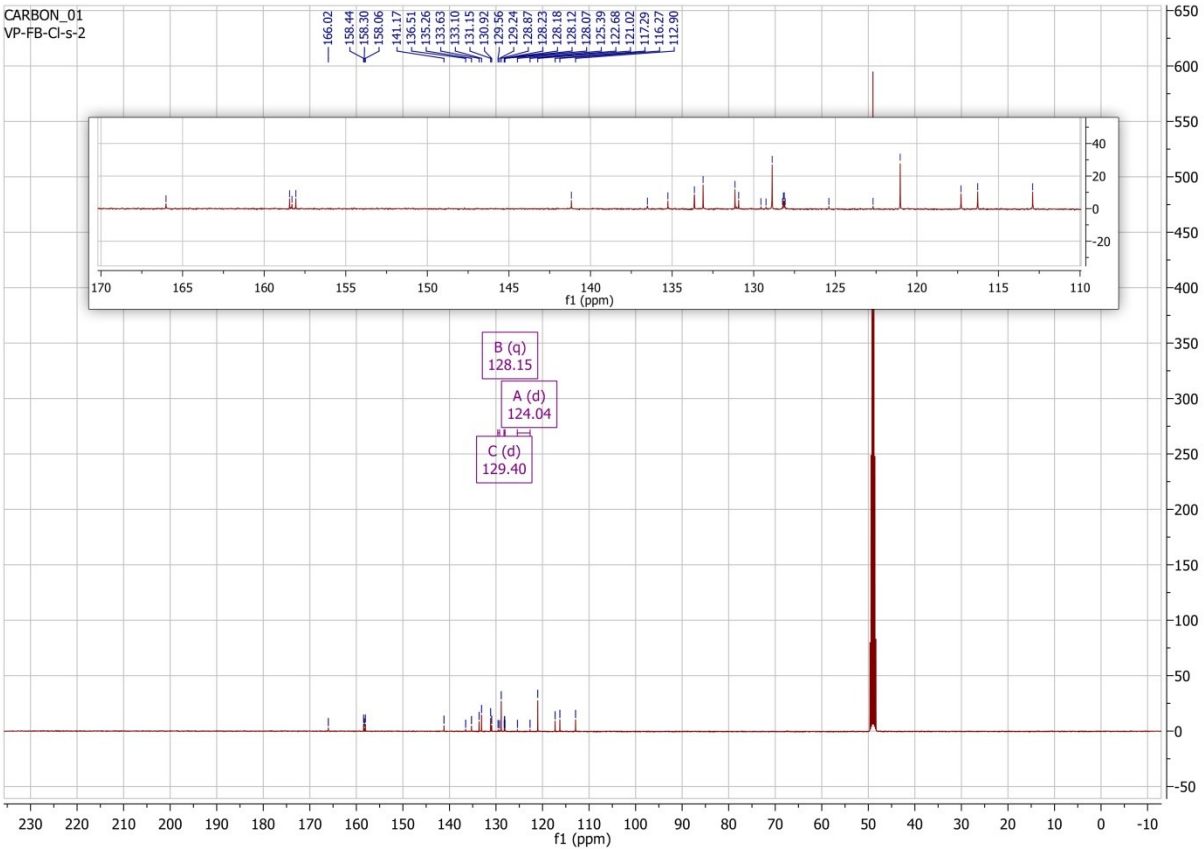

^{19}F-NMR (CD_3OD)

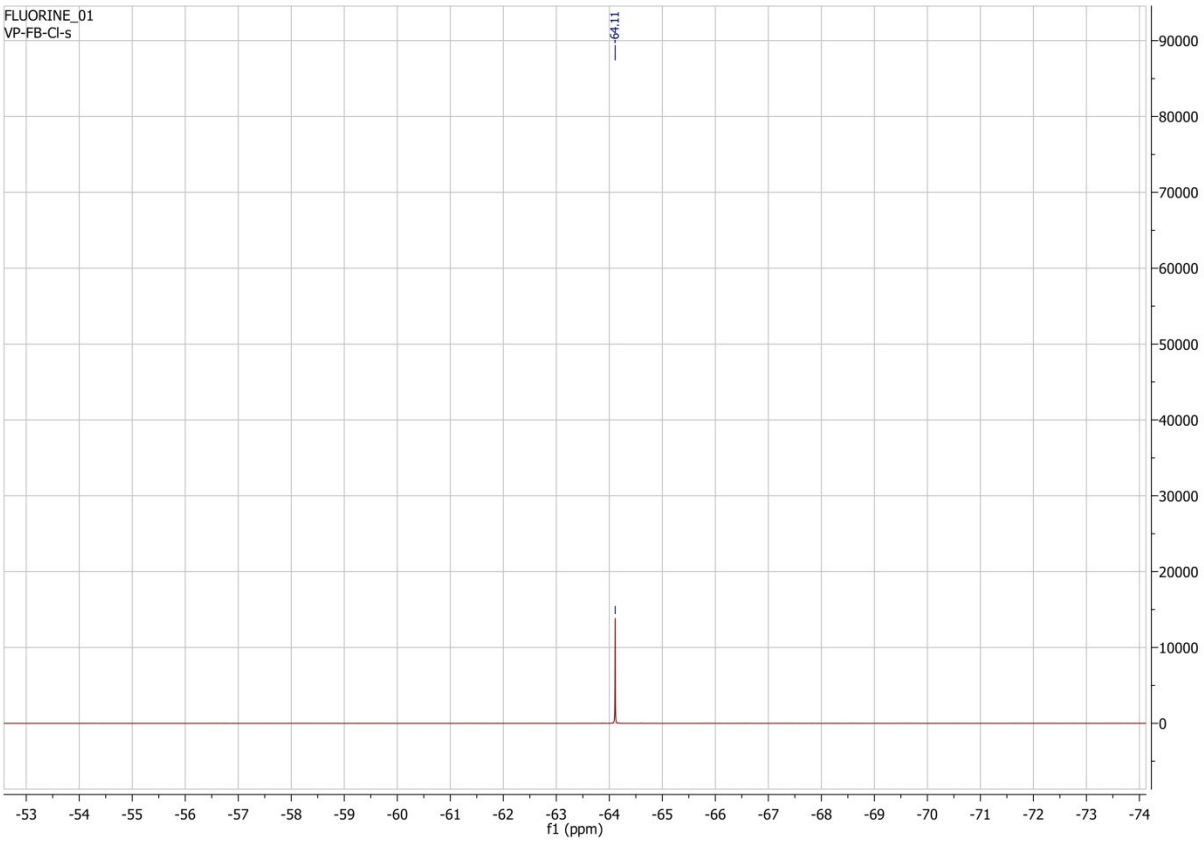

HPLC

Chromatogram : Gradient1_18_11_2014 12_38_49_channel1

System : HPLC-PDA
Method : Gradient1
User : Daniel

Acquired : 18/11/2014 12:43:32
Processed : 18/11/2014 13:31:01
Printed : 18/11/2014 17:31:14

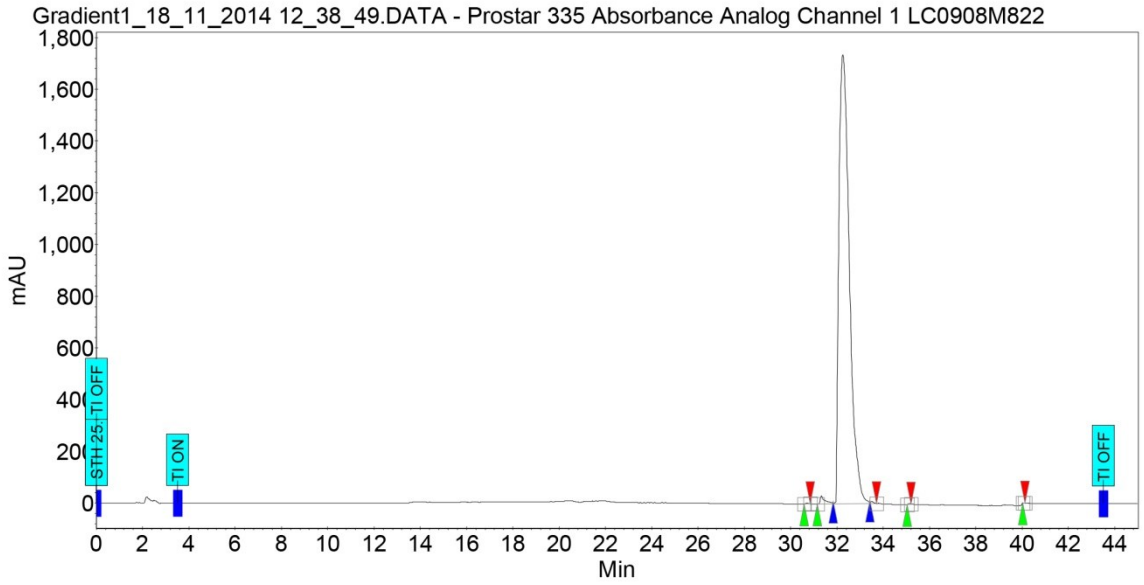

Peak results :

Index	Name	Time [Min]	Quantity [% Area]	Height [mAU]	Area [mAU.Min]	Area % [%]
1	UNKNOWN	30.72	0.05	3.7	0.4	0.047
2	UNKNOWN	31.32	0.90	31.9	8.2	0.895
3	UNKNOWN	32.25	98.91	1736.6	909.7	98.910
4	UNKNOWN	33.51	0.12	7.7	1.1	0.124
5	UNKNOWN	35.11	0.02	2.2	0.2	0.021
6	UNKNOWN	40.07	0.00	0.3	0.0	0.002
Total			100.00	1782.5	919.7	100.000

Compound 4:

^{1}H-NMR (CD_3OD)

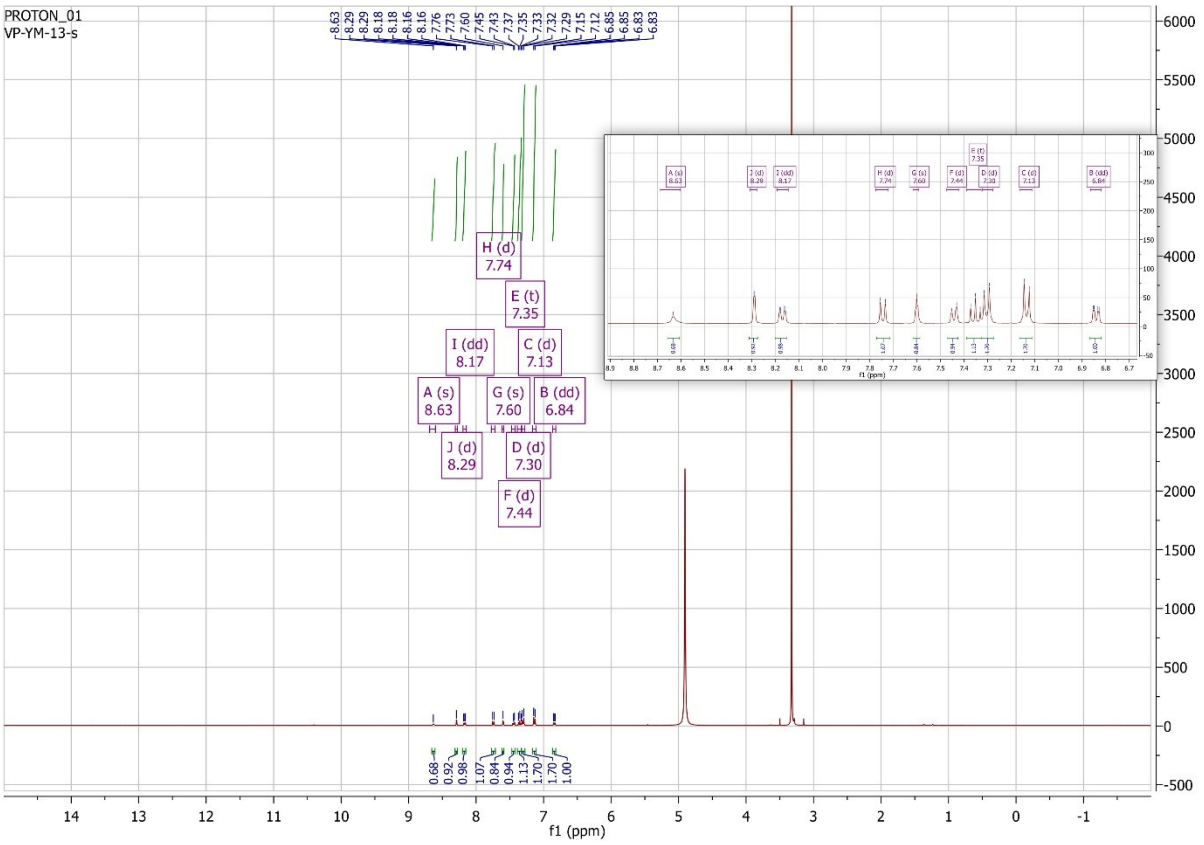

^{13}C-NMR (CD_3OD)

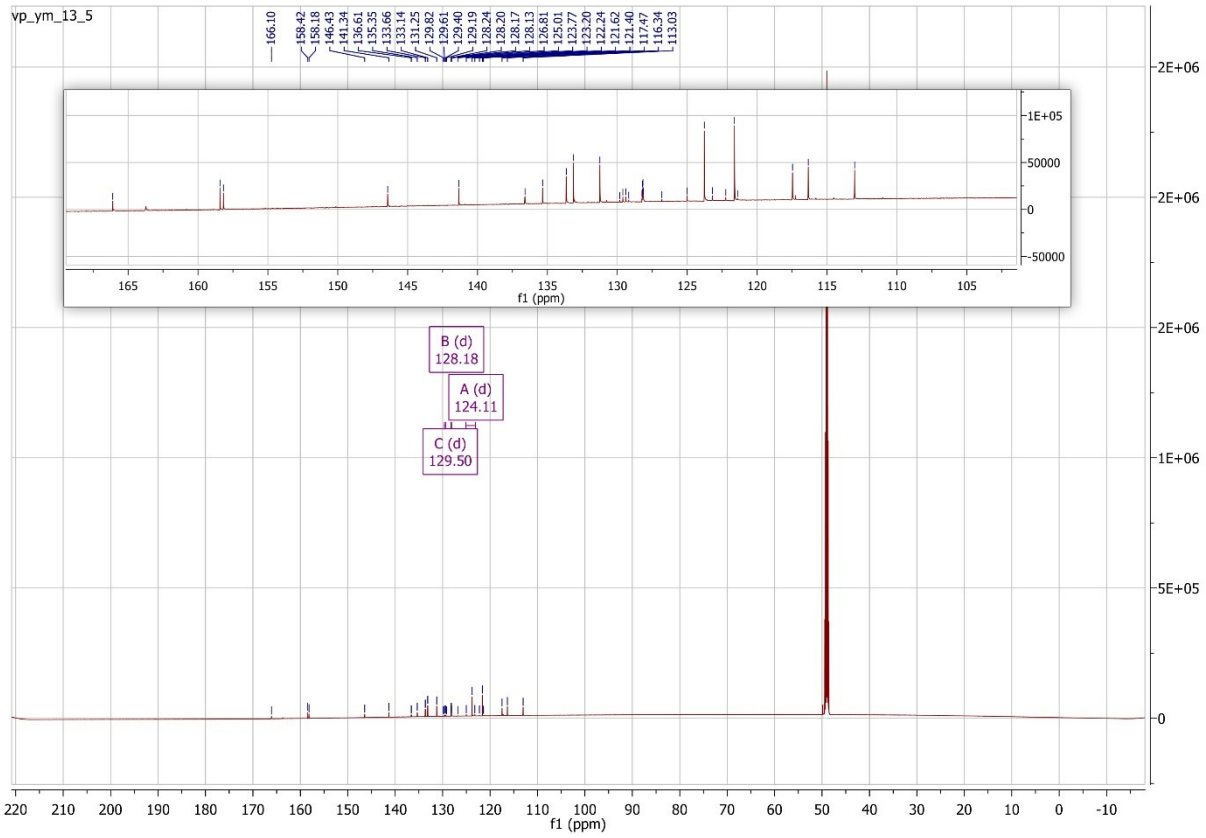

^{19}F-NMR (CD_3OD)

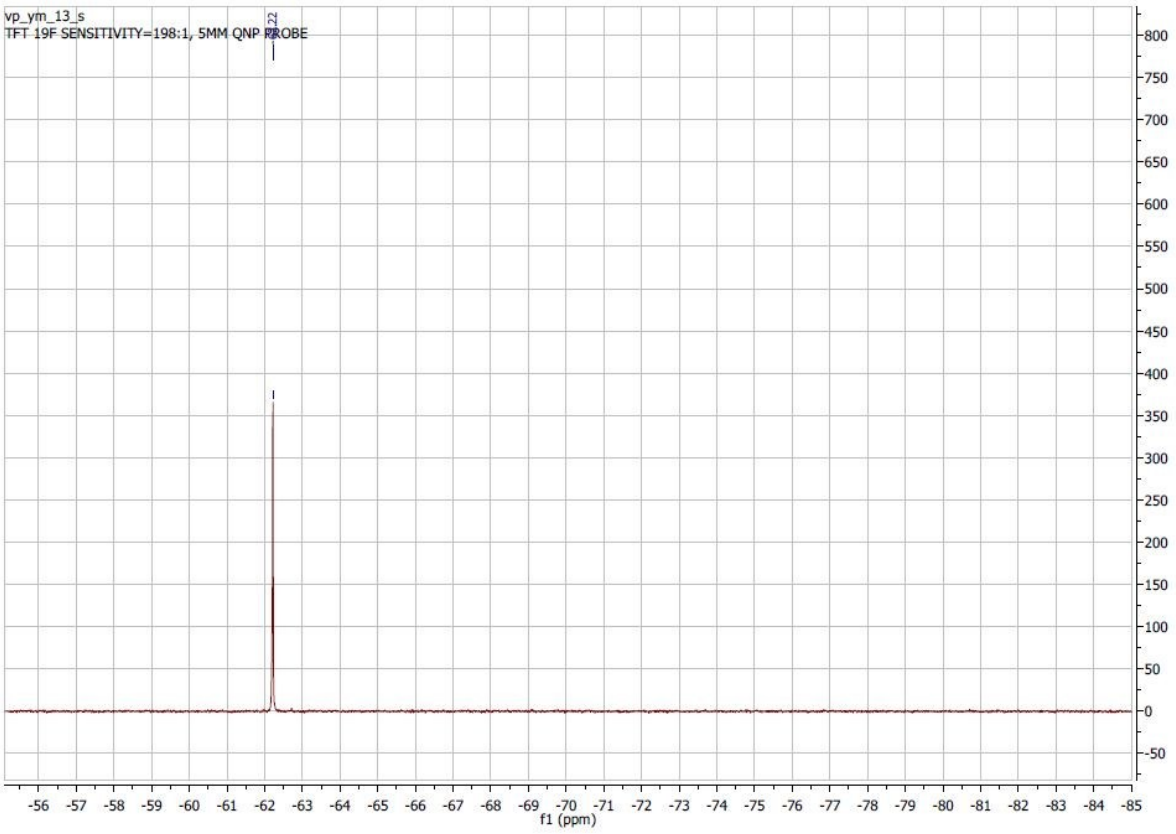

HPLC

Chromatogram : VP-YM-13-s_channel1

System : HPLC-PDA
Method : Gradient1
User : Daniel

Acquired : 04/09/2015 11:01:52
Processed : 04/09/2015 11:49:21
Printed : 04/09/2015 13:51:53

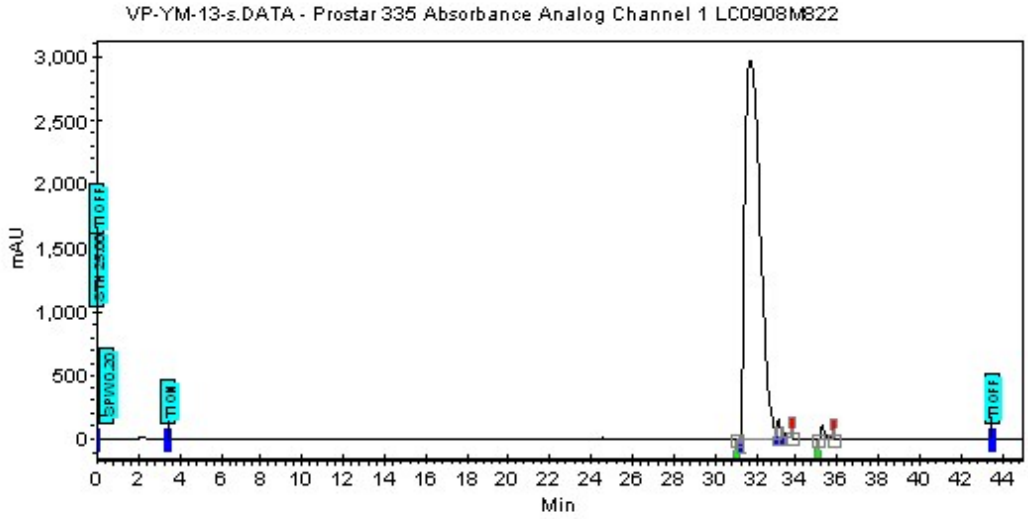

Peak results :

Index	Name	Time [Min]	Quantity [% Area]	Height [mAU]	Area [mAU.Min]	Area % [%]
1	UNKNOWN	31.17	0.02	5.8	0.7	0.023
2	UNKNOWN	31.72	97.69	2981.5	2710.2	97.686
3	UNKNOWN	33.15	0.99	147.9	27.3	0.986
4	UNKNOWN	33.36	0.43	61.1	11.9	0.428
5	UNKNOWN	35.28	0.88	111.3	24.3	0.877
Total			100.00	3307.6	2774.4	100.000

3. Calculated Properties

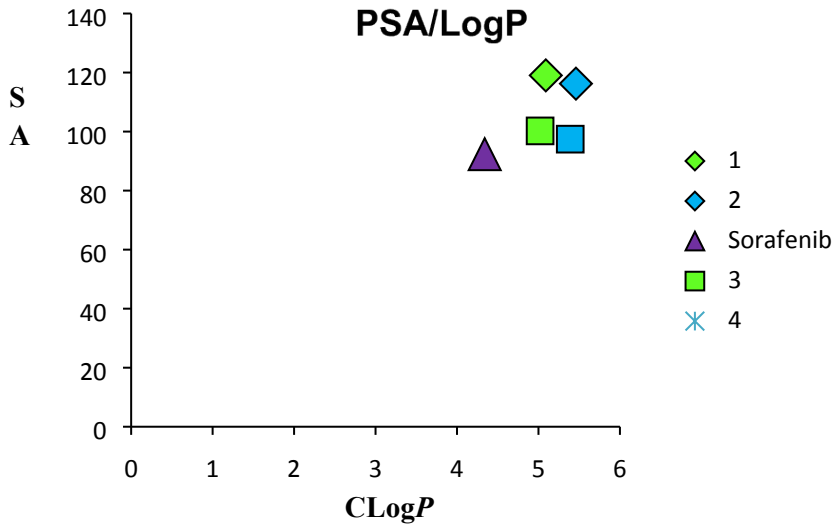

Figure S5. correlation between PSA (Å^2) and CLogP for compound **1**, **2**, **3**, **4** and sorafenib.

4. References

S1. C. Trujillo, V. Previtali, I. Rozas, A theoretical model of the interaction between phosphates in the ATP molecule and guanidinium systems, Theor. Chem. Acc., 135 (2016) 260.

S2. A.P. Kornev, N.M. Haste, S.S. Taylor, L.F. Eyck, Surface comparison of active and inactive protein kinases identifies a conserved activation mechanism, Proc. Natl. Acad. Sci. U.S.A., 103 (2006) 17783-17788.

S3. I. Rozas, On the nature of hydrogen bonds: an overview on computational studies and a word about patterns, Phys. Chem. Chem. Phys., 9 (2007) 2782-2790.

S4. D.H. O'Donovan, B. Kelly, E. Diez-Cecilia, M. Kitson, I. Rozas, A structural study of *N*,*N*′-bis-aryl-*N*″-acylguanidines, New J. Chem., 37 (2013) 2408-2418

S5. Y. Li, A. Urbas, Q. Li, Synthesis and characterization of light-driven dithienylcyclopentene switches with axial chirality, The Journal of organic chemistry, 76 (2011) 7148-7156.

S6. D. Maiti, S.L. Buchwald, Orthogonal Cu- and Pd-based catalyst systems for the O- and N-arylation of aminophenols, J Am Chem Soc, 131 (2009) 17423-17429.